

Fourth-generation Mobile Communication Using MIMO High-speed Packet Transmission

Hidekazu Taoka and Kenichi Higuchi†

Abstract

An ultrahigh-speed packet transmission experiment for achieving a transmission data rate of approximately 5 Gbit/s (spectral efficiency of 50 bit/s/Hz) was performed using a 100-MHz channel bandwidth in broadband packet radio access. The spectrum efficiency of 50 bit/s/Hz approaches the upper limit in cellular environments near a cell site, i.e., base station, taking into account inter-cell interference. This article gives an overview of the technology, describes the experimental configuration, and presents the results of a field experiment.

1. Introduction

The transmission data rate targeted by fourth-generation (4G) mobile communication systems called IMT-Advanced is 100 Mbit/s or greater in a cellular environment having a wide coverage area with high-mobility users and 1 Gbit/s or greater in an indoor or hotspot area with low-mobility users [1]. In previous field experiments using VSF-Spread OFDM*¹ radio access (VSF*²: variable spreading factor; OFDM*³: orthogonal frequency division multiplexing) with a channel bandwidth of 100 MHz, we achieved ultrahigh-speed packet transmission with a throughput*⁴ of 1 Gbit/s (spectral efficiency*⁵ of 10 bit/s/Hz). In those experiments, we used multiple-input multiple-output (MIMO) multiplexing consisting of four transmit/receive antennas at distances of up to 300 m from the base station under mostly non-line-of-sight conditions [2]. In Europe, the WINNER (Wireless World Initiative New Radio)*⁶ research forum has set the target value for peak spectral efficiency in an isolated cell environment as 25 bit/s/Hz as a system requirement for next-generation mobile communications

[3]. In this regard, we have also achieved an ultrahigh-speed packet transmission data rate of 2.5 Gbit/s (spectral efficiency of 25 bit/s/Hz) in an actual outdoor propagation environment featuring mobile terminal speeds of 5 to 20 km/h through the use of 6

Radio Access Network Development Department, NTT DOCOMO
Yokosuka-shi, 239-8536 Japan

† Currently also at the Department of Electrical Engineering, Faculty of Science and Technology at Tokyo University of Science

*1 VSF-Spread OFDM: A radio transmission method proposed by NTT DOCOMO that applies VSF*² to Spread OFDM*³. It is one of the candidates for increasing system capacity in the downlink cellular environment and in hotspot and indoor office environments for next-generation mobile communication systems.

*2 VSF: A technique that adaptively changes the spreading factor and channel coding rate in radio transmission methods that use data spreading such as W-CDMA (wideband code division multiple access) and Spread OFDM*³. VSF provides flexible support for various radio environments.

*3 Spread OFDM: OFDM is a digital modulation method that converts a high-data-rate signal into multiple low-speed narrowband signals and transmits them in parallel in the frequency domain to improve resistance to multipath interference and achieve high spectral efficiency. Spread OFDM is a radio transmission method that transmits the same signal using multiple subcarriers and time symbols to increase the received SINR*¹⁰ and suppress thermal noise and inter-cell interference.

*4 Throughput: The amount of data transmitted without error per unit time, i.e., the effective data transfer rate. In this article, throughput is defined as the (data rate on the transmission side) × (number of packets received without error per unit time) ÷ (number of packets transmitted per unit time).

*5 Spectral efficiency: The number of data bits that can be transmitted per unit time per unit bandwidth.

*6 WINNER: A European research forum concerned with radio transmission technology for next-generation mobile communications. Founded in 2004.

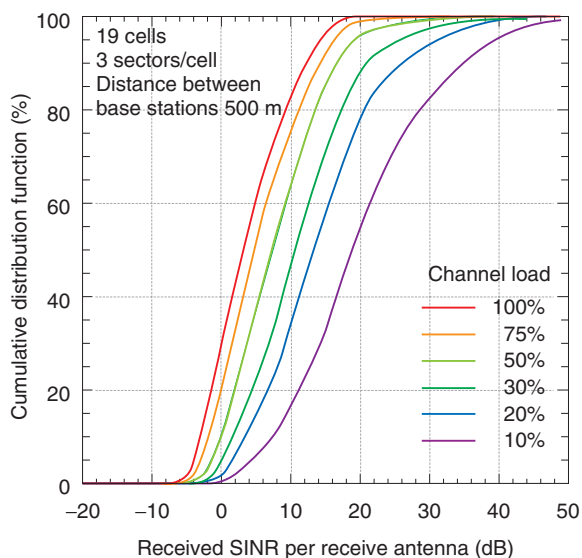


Fig. 1. Cumulative distribution function of received SINR in a cellular environment.

transmit/receive antennas, 64QAM (quadrature amplitude modulation)^{*7}, and turbo coding^{*8} with a channel coding rate^{*9} of $R = 8/9$ [4].

In packet transmission, the maximum transmission data rate typically corresponds to the peak throughput per cell. It is therefore important that we investigate the maximum achievable transmission data rate since raising the maximum transmission data rate for one user increases the number of users that can be accommodated by high-speed transmission. In a completely isolated cell environment in which interference from neighboring cells is nonexistent, the maximum transmission data rate can be raised without limit by increasing the number of transmit/receive antennas and the transmission power. In a multi-cell environment, however, increasing the number of antennas and transmission power also increases the amount of interference from neighboring cells. The maximum achievable transmission data rate is therefore determined by the received signal-to-interference-plus-noise-power ratio (SINR)^{*10}, which takes inter-cell

interference into account. We simulated a multi-cell environment with 19 cells (3 sectors per cell) with base station transmission power of 20 W and a distance between base stations of 500 m with the volume of traffic in neighboring cells (channel load) as a parameter. The cumulative distribution function of received SINR obtained from this simulation is shown in **Fig. 1**. These results show that the distribution of received SINR improves as channel load becomes smaller. But it can also be seen that received SINR at nearly all locations within a cell is no more than approximately 30 dB even in the case of a small channel load. We can therefore consider the maximum received SINR in a cellular environment to be approximately 30 dB, assuming a low-channel-load case. By performing computer simulations under the condition of a received SINR of 30 dB, we found that spectral efficiency of approximately 50 bit/s/Hz can be achieved.

In this article, we give an overview of the technology, describe the experimental configuration, and present the results of an ultrahigh-speed packet transmission field experiment using VSF-Spread OFDM radio access with a 100-MHz channel bandwidth for achieving a transmission data rate of approximately 5 Gbit/s (spectral efficiency of 50 bit/s/Hz), which is practically the ultimate data rate taking into account the inter-cell interference.

2. Technologies for 50-bit/s/Hz ultrahigh spectral efficiency

We applied the following technologies for achieving ultrahigh spectral efficiency of approximately 50 bit/s/Hz.

- 1) MIMO multiplexing with 12 transmit/receive antennas
- 2) 64QAM and turbo coding with a channel coding rate of $R = 8/9$
- 3) Signal separation algorithm based on maximum likelihood detection (MLD)^{*11}

The application of technologies 1) and 2) resulted in a transmission data rate of 4.915 Gbit/s (excluding

*7 64QAM: A digital modulation method in wireless communications that transmits data using 64 different phase and amplitude constellations. It can transmit 6 bits per symbol, surpassing quadrature phase shift keying (QPSK) and 16QAM.

*8 Turbo coding: A type of error correction coding that achieves powerful error-correction performance through iterative decoding using reliability information in decoded results.

*9 Channel coding rate: The ratio of the number of data bits to the number of bits after error correction coding (a coding rate of 8/9 means that 8 bits of data become 9 bits after error correction coding has been performed).

*10 Received SINR: Ratio of the power of the desired received signal to the sum of the powers of other received signals (interfering signals from other cells or sectors and thermal noise).

*11 MLD: A method of signal separation in MIMO multiplexing. Using the received signals of all the receive antenna branches, this method selects the most likely combination of signal points from among all possible signal-point candidates in the digital modulation (64QAM in this article) of each transmit antenna branch.

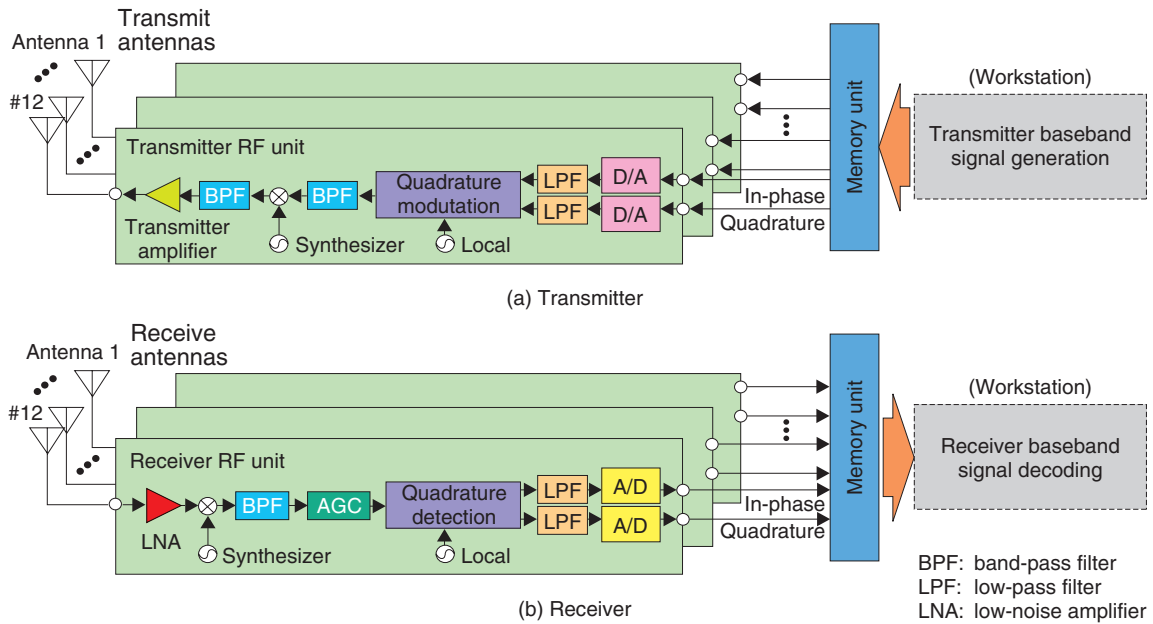


Fig. 2. Configuration of MIMO transmitter/receiver experimental equipment.

the pilot signal and other overheads) in OFDM radio access with a channel bandwidth of 100 MHz. The application of high-accuracy signal separation technology 3) could significantly decrease the required received SINR compared with other signal separation methods.

In this signal separation method, to reduce the computational complexity of MLD, which is particularly high when a higher data modulation scheme is used, we applied adaptive selection of surviving symbol replica candidates (ASESS)^{*12} [5], a method that we previously proposed using reliability information of symbol replica candidates^{*13}, to complexity-reduced MLD with QR decomposition^{*14} and the M-algorithm^{*15} (QRM-MLD)^{*16} [6]. The QRM-MLD method using ASESS can greatly reduce computational complexity with almost no deterioration in throughput. This is achieved by decreasing the number of

Euclidean distance^{*17} calculations required for signal separation by using reliability information for each symbol obtained simply by symbol^{*18} ranking using quadrant detection^{*19}.

When a transmission data rate of 5 Gbit/s is achieved using radio transmission technologies 1) to 3) above, QRM-MLD with ASESS can reduce the computational complexity to approximately $1/(2 \times 10^{17})$ times that of MLD without computation-reduction measures and to approximately 1/15 that of the original QRM-MLD method.

3. Structure of MIMO multiplexing transceivers

The configuration of the experimental transmitter and receiver equipment that we constructed is shown in Fig. 2. The carrier frequency and bandwidth are 4.635 GHz and 101.4 MHz, respectively. Each trans-

*12 ASESS: A method for sequentially selecting symbol replica candidates with high reliability based on the reliability information and accumulated branch metric of each symbol obtained by simple symbol ranking using quadrant detection^{*19}.

*13 Symbol replica candidate: Possible signal-point candidate of each transmit antenna branch. It is the received signal-point candidate calculated using the estimated amount of fluctuation in channel amplitude and phase.

*14 QR decomposition: A mathematical technique for decomposing any m -row \times n -column complex matrix H into the product of $m \times n$ unitary matrix Q and $n \times n$ upper triangular matrix R ($H=QR$).

*15 M-algorithm: A method for successively reducing symbol candidates at each stage (transmit antenna) by selecting M ($\leq N$) out of N symbol replica candidates.

*16 QRM-MLD: As in MLD, this method selects the most likely combination of signal points from among all possible signal-point candidates of each transmit antenna branch. The application of QR decomposition and the M-algorithm significantly reduces the computational complexity.

*17 Euclidean distance: The shortest distance between two points in space.

*18 Symbol: In this article, the signal unit after error correction coding and data modulation mapping.

*19 Quadrant detection: On the xy plane, a method for detecting in which of four quadrants delimited by the x and y axes centered on the origin an entity is positioned. Quadrant detection in this article is easily performed by simply detecting the in-phase and the quadrature components of the received signal.

Table 1. Basic specifications of RF unit.

Carrier frequency	4.635 GHz
Bandwidth	101.4 MHz
No. of antennas	12 (transmit/receive)
Base station transmission power	20 W (total)
No. of quantized bits in converters	14 bit (D/A), 12 bit (A/D)
Sampling clock rate	270 Msample/s
Memory (per branch)	9 Gbyte (transmitter), 18 Gbyte (receiver)
Hard disk capacity	480 Gbyte

memory unit and radio unit, the latter including a digital-to-analog (D/A) (analog-to-digital (A/D)) converter. In this experimental system, transmitted signal generation before the D/A conversion at the transmitter and received signal demodulation after A/D conversion at the receiver are done offline by a workstation. However, because actual radio-frequency (RF) transceivers are used for the signal transmission, the transmission performance is the same as for realtime signal transmission. The basic specifications of the RF unit are given in **Table 1** and those of the baseband signal processing unit are given in **Table 2**.

The transmitter consists of a workstation equipped with a 480-Gbyte hard disk, a memory unit with 9 Gbyte of memory per branch^{*20}, a 14-bit D/A converter, intermediate frequency (IF)^{*21} and RF transmission circuits, and 12 branches of transmit antennas. First, the workstation turbo codes and bit interleaves^{*22} the binary information bit sequence (constraint length^{*23} = 4 bits; $R = 8/9$) and then performs 64QAM data modulation mapping. It then applies a serial-to-parallel conversion to the transmit symbol sequence resulting from data modulation, placing it onto 1536 subcarriers. Next, it time-multiplexes

*20 Branch: In this article, an antenna and RF transmitter or receiver.

*21 IF: In a radio receiver circuit, specific frequencies used for improving frequency selectivity and receiver sensitivity. Although a variety of radio frequencies are used in mobile communication systems, they are commonly converted to IF before demodulation within receiver circuits.

*22 Interleaving: In this article, a technique for randomizing burst errors caused by fluctuation in fading in mobile communications. The combination of interleaving and error correction coding raises error correction performance. Interleaving performed on a bit sequence before data modulation is called bit interleaving. Deinterleaving means returning the randomized transmit signal to its original order at the receiver.

*23 Constraint length: Number of past input bits needed to obtain the output. A longer constraint length improves error correction performance but increases the computation required for decoding.

Table 2. Basic specifications of baseband signal processing unit.

Radio access	VSF-Spread OFDM
Subframe length	0.5 ms
No. of subcarriers	1536 (subcarrier separation: 65.919 kHz)
OFDM symbol duration	Data 15.170 μ s + CP 2.067 μ s
Spreading factor	1
Channel coding, decoding;	Turbo coding ($R=8/9$, $K=4$), Max-log-MAP decoding
Window timing detection	Pilot symbol-based window timing detection
Channel estimation	2D MMSE channel estimation filter
Signal separation method	QRM-MLD with ASESS

quadrature pilot symbols^{*24} characteristic of the transmit antennas into subframes (subframe length: 0.5 ms) and generates a symbol sequence for each transmit antenna. The symbol sequence is converted to OFDM symbols (effective symbol length: 15.170 μ s) by a 2048-point inverse fast Fourier transform (IFFT)^{*25} and adds a cyclic prefix (CP)^{*26} with a duration of 2.067 μ s. The baseband modulated signal of the in-phase and quadrature components^{*27} after CP insertion is now stored in the memory unit of the transmitter. D/A conversion is applied to the transmitted signals at a sampling rate of 270 Msample/s followed by quadrature modulation, conversion to an RF signal, and transmission from each antenna.

The receiver consists of 12 branches of receive antennas, RF and IF receiver circuits, a 12-bit A/D converter, 18 Gbyte of memory per branch, and a workstation equipped with a 480-Gbyte hard disk. In the IF band, the received signals are linearly amplified by an automatic gain control (AGC) amplifier, and then quadrature detection and A/D conversion are performed. The baseband modulated received signal of the in-phase and quadrature components is now stored in the receiver's large-capacity memory. Next, the workstation takes this digital signal and performs

*24 Pilot symbol: A symbol that is known to both the transmitter and receiver. Used on the receiver side for synchronizing symbols, estimating amplitude and phase fluctuation on the channel, and estimating the received signal power, interference power, and noise power.

*25 IFFT: Inverse fast Fourier transform (inverse of FFT^{*28}). Generates a temporal waveform signal by convoluting the signals of all the frequency components.

*26 CP: A guard interval inserted between OFDM symbols to eliminate inter-symbol interference and adjacent-subcarrier interference caused by multipath delay.

*27 Baseband modulated signal of the in-phase and quadrature components: the in-phase and quadrature components of the digital signal before quadrature modulation (after detection).

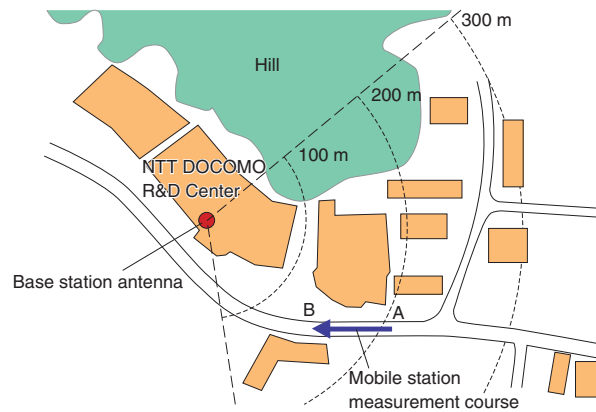


Fig. 3. Measurement course for field experiment.

fast Fourier transform (FFT)^{*28} window-timing^{*29} detection. Then, after performing CP removal, it separates the signal into the components of each sub-carrier. Following this, the channel estimation value^{*30} for each subcarrier is estimated by two-dimensional minimum mean square error (MMSE) channel estimation^{*31} [7], and in the signal-separation unit, signal detection is performed by QRM-MLD with ASESS using these channel estimation values. Next, to perform soft-decision^{*32} turbo decoding, the workstation calculates a log likelihood ratio (LLR)^{*33} [8] for each bit from the signal output from the signal-separation unit, and after performing deinterleaving^{*22}, it inputs the signal into a turbo decoder (max-log-MAP decoding)^{*34} and recovers the transmit signal sequence.

*28 FFT: A technique for quickly extracting the frequency components and their power ratios included in a signal.

*29 Window timing: Receive timing for performing an FFT.

*30 Channel estimation value: The amount of fluctuation in the propagation path (channel) estimated using pilot symbols time-multiplexed with data symbols within each packet frame.

*31 Two-dimensional MMSE channel estimation: Taking the correlation between channel fluctuation in the temporal and frequency directions into account and using pilot symbols multiplexed within fixed subcarrier intervals and time intervals, this technique performs high-accuracy estimation of frequency-and-temporal channel fluctuation in data symbols multiplexed between the pilot symbols in a way that minimizes the estimation error.

*32 Soft-decision: A type of decoding that adds reliability information to received symbols and uses the value itself of the received signal based on that information. Compared with a hard-decision, which decodes the received signal into a binary result (0 or 1), a soft-decision achieves higher error correction performance.

4. Field experiment results

The field experiment was conducted on the measurement course, shown in **Fig. 3**, located in the Yokosuka Research Park district of Yokosuka City, Kanagawa prefecture, Japan. The base station antennas and the measurement van equipped with mobile station antennas used in the field experiment are shown in **Photo 1**. The transmit antenna at the base station was a 12-branch sectored-beam antenna^{*35} with a 3-dB width of 90° in azimuth installed at a height of approximately 26 m. The transmission power and antenna gain of each antenna were 20 W and 19 dBi, respectively, and antennas were linearly arranged with an adjacent antenna separation of 70 cm (equivalent to approximately 11 wavelengths for the carrier frequency of 4.635 GHz). The mobile station used 12 dipole antennas^{*36} installed in a row at a height of approximately 3.5 m. The antenna gain was 2 dBi and the separation between adjacent receive antennas was set to 20 cm (equivalent to approximately 3.1 wavelengths). In the experiment, the van

*33 LLR: Used in soft-decision decoding. The logarithm of the ratio of reliability information (likelihood) of the required received data being 0 to the reliability information (likelihood) of the data being 1.

*34 Max-log-MAP decoding: A channel decoding algorithm. Compared with maximum a posteriori probability (MAP), which is considered to be an optimal decoding algorithm, max-log-MAP achieves nearly equivalent characteristics with significantly less computational complexity by using an approximation in the calculation of a posteriori probability.

*35 Sectored-beam antenna: An antenna with directional properties used for reducing interference between adjacent sectors of a sectored base station.

*36 Dipole antenna: The simplest of all antennas, comprising two straight, linearly aligned conductor wires (elements) attached to the end of a cable (feed point).

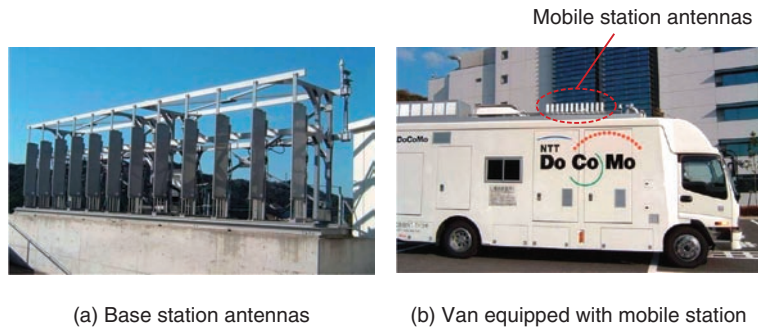
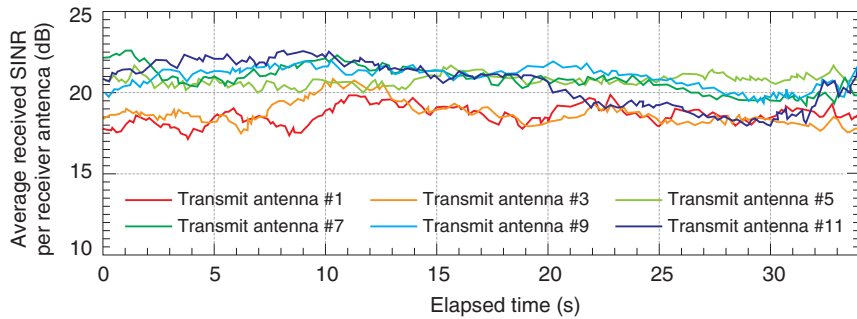
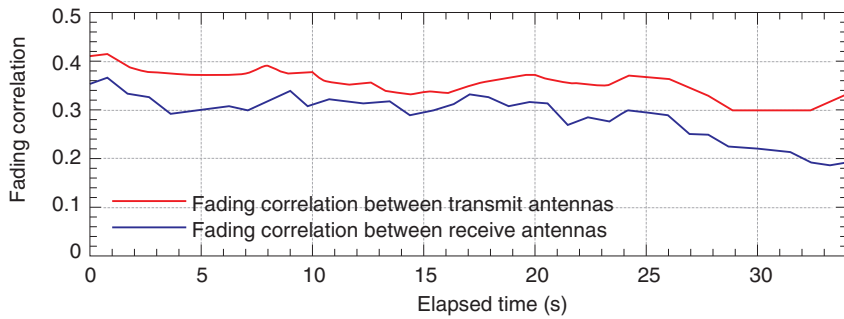


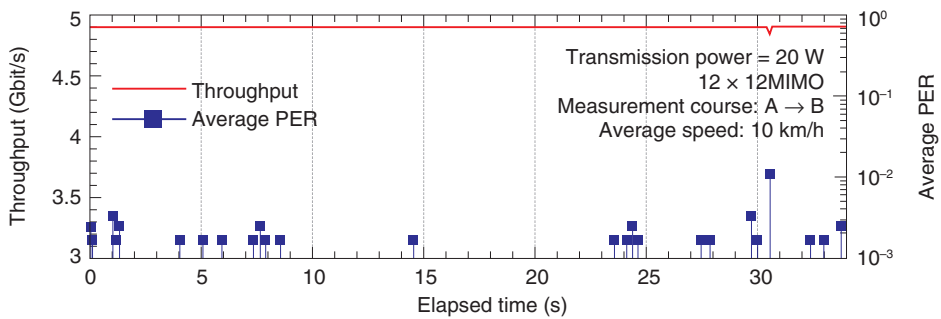
Photo 1. Base station antennas and mobile station measurement van.



(a) Received SINR



(b) Fading correlation



(c) Throughput/average-PER

Fig. 4. Time variation performance.

was driven along the measurement course at an average speed of approximately 10 km/h, and the distance from the transmitter ranged from 150 to 200 m. The majority of the course was in the non-line-of-sight condition because there were office buildings, approximately three to six stories high, between the transmitter and receiver.

The time variations in the average total received SINR per receive antenna, the measured fading correlations between adjacent transmit antennas, and the average packet error rate (PER) along with the measured throughput using 12×12 MIMO multiplexing are shown in Fig. 4. Figures 4(a) and (b) reveal that the received SINR per transmit antenna fluctuated in the range from approximately 18 to 22 dB and that the variation in the measured fading correlation over the course was small: in the range of approximately 0.2 to 0.4. Figure 4(c) clearly shows that 4.915-Gbit/s packet transmission with an average PER below 10^{-2} was achieved at most of the locations along the measurement course, where the maximum distance from the base station was approximately 200 m. The measured throughput using 12×12 MIMO multiplexing as a function of the average total received SINR with a receive antenna spacing of 20 cm is shown in Fig. 5. The computer simulation results are also shown assuming a propagation channel condition corresponding to the average value of delay spread^{*37} and fading correlation between antennas along the measurement course in the field experiment. From the figure, we can see that the difference in the required received SINR between the results of the field experiment and those of simulation is less than 1 dB. The deviation is mainly due to the difference in the propagation channel model, channel estimation error, and signal detection error caused by quantization error in the A/D converter of the implemented MIMO receiver. Figure 5 also shows that peak throughput of 4.915 Gbit/s, i.e., frequency efficiency of approximately 50 bit/s/Hz, was achieved at an average total received SINR per receive antenna of approximately 28.5 dB when the receive antenna spacing was 20 cm by adopting the QRM-MLD signal detection method with ASESS.

*37 Delay spread: For radio propagation in mobile communications, the spread in delay time of all paths (waves) arriving late because of reflection or diffraction from buildings or other objects. Defined by the standard deviation determined by weighted statistical processing of the delay time of all arriving paths (waves) using the received signal power.

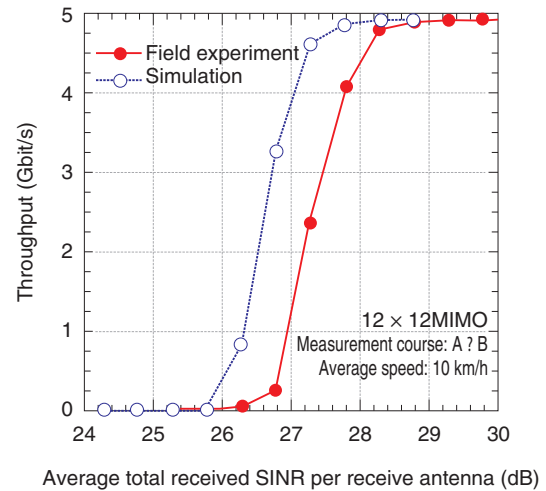


Fig. 5. Throughput performance.

5. Conclusion

We described the technology behind an ultrahigh-speed packet transmission field experiment using VSF-Spread OFDM radio access for achieving a maximum transmission data rate of approximately 5 Gbit/s with 100-MHz channel bandwidth and presented field experimental results. Using MIMO multiplexing consisting of 12 transmit/receive antennas in an actual outdoor propagation environment, we showed that ultrahigh-speed packet transmission with a maximum throughput of approximately 5 Gbit/s (spectral efficiency of approximately 50 bit/s/Hz) could be achieved with a required average total received SINR of approximately 28.5 dB.

References

- [1] ITU-R Recommendation M.1645.
- [2] H. Taoka, K. Higuchi, and M. Sawahashi, "Field Experiments on Real-Time 1-Gbps High-Speed Packet Transmission in MIMO-OFDM Broadband Packet Radio Access," Proc. of the 63rd IEEE VTC2006-Spring, Vol. 4, pp. 1812–1816, Melbourne, Australia, 2006.
- [3] IST-2003-507581, D7.1 v1.0, System Requirements, WINNER, July 2004.
- [4] H. Taoka, K. Dai, K. Higuchi, and M. Sawahashi, "Field Experiments on 2.5-Gbps Packet Transmission Using MLD-based Signal Detection in MIMO-OFDM Broadband Packet Radio Access," Proc. of the 9th WPMC2006, pp. 234–239, San Diego, USA, 2006.
- [5] K. Higuchi, H. Kawai, N. Maeda, and M. Sawahashi, "Adaptive Selection of Surviving Symbol Replica Candidates Based on Maximum Reliability in QRM-MLD for OFCDM MIMO Multiplexing," Proc. of IEEE Globecom 2004, pp. 2480–2486, Dallas, Texas, USA, 2004.
- [6] K. -J. Kim, J. Yue, R. A. Iltis, and J. D. Gibson, "A QRD-M/Kalman filter-based detection and channel estimation algorithm for MIMO-OFDM systems," IEEE Trans. on Wireless Commun., Vol. 4, No. 2, pp. 710–721, 2005.

- [7] O. Edfors, M. Sandell, J.-J. Beek, S. Kate, and P. O. Borjesson, "OFDM channel estimation by singular value decomposition," *IEEE Trans. Commun.*, Vol. 46, No.7, pp. 931–939, 1998.
- [8] K. Higuchi, H. Kawai, N. Maeda, M. Sawahashi, T. Itoh, Y. Kakura,

A. Ushirokawa, and H. Seki, "Likelihood function for QRM-MLD suitable for soft-decision turbo decoding and its performance for OFCDM MIMO multiplexing in multipath fading channel," *Proc. of IEEE PIMRC 2004*, pp. 1142–1148, Sep. 2004.



Hidekazu Taoka

Assistant Manager, Radio Access Network Development Department, NTT DOCOMO.

He joined NTT DOCOMO in 2000 and engaged in R&D of radio access technology for Super 3G and 4G mobile communication systems. He is a member of the Institute of Electronics, Information and Communication Engineers (IEICE) of Japan.



Kenichi Higuchi

Assistant Manager, Radio Access Network Development Department, NTT DOCOMO.

He received the Dr.Eng. degree. He joined NTT Mobile Communications Network (now NTT DOCOMO) in 1994 and engaged in R&D of wireless access technology for W-CDMA, Super 3G, and 4G mobile communications systems. Since 2007, he has also been serving in the Department of Electrical Engineering, Faculty of Science and Technology, at Tokyo University of Science. He is a member of IEEE and IEICE.
